International Journal of Bifurcation and Chaos, Vol. 31, No. 5 (2021) 2130014 (17 pages)

DOI: 10.1142/S0218127421300147

Coexisting Infinite Equilibria and Chaos

Chunbiao Li[*,†,§], Yuxuan Peng[†,‡,¶] and Ze Tao[†,‡,‖]
[*]*School of Artificial Intelligence,*
Nanjing University of Information Science and Technology,
Nanjing 210044, P. R. China
[†]*Jiangsu Collaborative Innovation Center of Atmospheric Environment and Equipment Technology (CICAEET),*
Nanjing University of Information Science and Technology,
Nanjing 210044, P. R. China
[‡]*Jiangsu Key Laboratory of Meteorological Observation and Information Processing, Nanjing University of Information Science and Technology, Nanjing 210044, P. R. China*
[§]*goontry@126.com*
[§]*chunbiaolee@nuist.edu.cn*
[¶]*alexpengcn@foxmail.com*
[‖]*lebrontaoze@163.com*

Julien Clinton Sprott
Department of Physics,
University of Wisconsin−Madison,
Madison, WI 53706, USA
sprott@physics.wisc.edu

Sajad Jafari
Biomedical Engineering Faculty,
Amirkabir University of Technology,
424 Hafez Ave, 15875-4413, Tehran, Iran
sajadjafari83@gmail.com

Received March 18, 2020; Revised October 18, 2020

Equilibria are a class of attractors that host inherent stability in a dynamic system. Infinite number of equilibria and chaos sometimes coexist in a system with some connections. Hidden chaotic attractors exist independent of any equilibria rather than being excited by them. However, the equilibria can modify, distort, eliminate, or even instead coexist with the chaotic attractor depending on the distance between the equilibria and chaotic attractor. In this paper, chaotic systems with infinitely many equilibria are considered and explored. Extra surfaces of equilibria are introduced into the chaotic flows, showing that a chaotic system can maintain its basic dynamics if the newly added equilibria do not intersect the original attractor. The offset-boostable plane of equilibria rescales the frequency of the chaotic oscillation with an almost linearly modified largest Lyapunov exponent or conversely drives the system into periodic oscillation, even ending in a divergent state. Furthermore, additional infinite number of equilibria or even a solid space of equilibria are safely nested into the chaotic system without destroying

[§]Author for correspondence

the original dynamics, which provides an alternate permanent location for a dynamical system. A circuit simulation agrees with the numerical calculation.

Keywords: Chaotic attractor; infinite equilibria; offset boosting.

1. Introduction

Equilibrium points play an important role in nonlinear dynamical systems, which drive the system into various states. However, it appears that chaotic attractors can be independent of the equilibria in the case of a hidden attractor [Leonov & Kuznetsov, 2013a; Leonov *et al.*, 2011, 2012, 2015; Zhang & Wang, 2019a]. Chaos exists in dynamical systems with no equilibria [Zhou *et al.*, 2018; Jafari & Sprott, 2013a; Maaita *et al.*, 2015; Akgul *et al.*, 2016; Jafari *et al.*, 2016a], with only stable equilibria [Molaie & Jafari, 2013; Wang & Chen, 2013; Deng & Wang, 2019; Li & Sprott, 2013; Yang & Chen, 2008], with line equilibria [Ma *et al.*, 2015; Li *et al.*, 2014; Jafari & Sprott, 2013b; Li & Sprott, 2014; Li *et al.*, 2015b], with planes of equilibria [Ekmekci & Rockwell, 2010; Bao *et al.*, 2017; Jafari *et al.*, 2016b; Li & Sprott, 2017; Macbeath, 1965], or even with any number of equilibria [Wang & Chen, 2013]. Even when unstable equilibria exist, the initial condition in the neighborhood of the equilibria may instead lead to an alternate third chaotic state [Li *et al.*, 2017a; Li *et al.*, 2015a]. All of the chaotic attractors identified in the above cases are hidden attractors [Leonov & Kuznetsov, 2013b; Leonov *et al.*, 2015; Zhang & Wang, 2019a]. These hidden chaotic attractors share a common feature in that their basins of attraction do not cover or cross the neighborhood of the existing equilibria. Furthermore, chaos can coexist with infinitely many equilibrium points when a periodic function is introduced to construct infinitely many attractors based on initial-condition-based offset boosting [Kuznetsov *et al.*, 2013; Bao *et al.*, 2016; Li *et al.*, 2018b; Lai & Chen, 2016; Zhang & Wang, 2019b].

Chaotic systems with surfaces of equilibria have various mechanisms, some of which are induced by dimension redundancy [Bao *et al.*, 2017], a preconstraint [Jafari *et al.*, 2016b], or even time rescaling [Li & Sprott, 2017]. In fact, function-based time rescaling produces a mixed effect of frequency modification and bifurcation control when the surfaces of equilibria are introduced by a function. Chaotic systems with surfaces of equilibria have other possibilities for hosting infinitely many equilibrium points, including other types of surfaces, lines of equilibria, and even a solid space of equilibria if they do not intersect or conflict with the previously existing attractors. In this paper, from the newly found chaotic flows with surfaces of equilibria [Jafari *et al.*, 2016c], additional cases with infinitely many equilibrium points are derived and explored when new functions are introduced. In Sec. 2, the derived chaotic systems with surfaces of equilibria are listed with a basic dynamical analysis. In Sec. 3, from a systematic bifurcation analysis, it is shown that the newly introduced functions cause a time rescaling, and the fundamental dynamics of those cases with infinitely many equilibria depend on the core system rather than the newly attached equilibria. Electrical circuit simulation described in Sec. 4 confirms the findings from numerical simulation. A discussion and conclusion are presented in the last section.

2. Chaotic Systems with Infinite Equilibria

Based on the newly found simplest chaotic flows with surfaces of equilibria [Jafari *et al.*, 2016c], additional surfaces are considered to introduce extra equilibria, as shown in Table 1. Here, to employ a compatible differential equation, the function f_{i0} represents the original flows proposed in the reference [Jafari *et al.*, 2016c], while f_{ij} are the functions added to construct other chaotic systems with new surfaces of equilibria. The Lyapunov exponents and Kaplan–Yorke dimensions are calculated from initial conditions close to the attractor, which are close to those of the original chaotic systems. In the reference [Jafari *et al.*, 2016c], an exhaustive computer search was performed to seek elegant dissipative cases for which the largest Lyapunov exponent is greater than 0.001, where the simplest candidates for the surface $f(x, y, z)$ are simple planes (a single plane, two orthogonal planes or even three orthogonal planes) or other standard quadrics (ellipsoids, hyperboloids, and paraboloids). In Table 1, we show that different equilibria can be introduced into the

Table 1. Chaotic systems with surfaces of equilibria.

Cases	System Structure	Introduced Functions	Surfaces of Equilibria	LEs	D_{KY}	(x_0, y_0, z_0)
ES1	$\dot{x} = f_{ij} \times (y)$ $\dot{y} = f_{ij} \times (z)$ $\dot{z} = f_{ij} \times (-x + ay^2 - xz)$ $a = 1.54$	$f_{10} = x$ (ES1a)	$(0, y, z)$	0.0071 0 −1.0864	2.0065	6 0 −1
		$f_{11} = 1 + x^2 - y^2$ (ES1b)	$y^2 - x^2 = 1$	0.0394 0 −6.0477	2.0065	
		$f_{12} = z + x^2 + y^2$ (ES1c)	$x^2 + y^2 = -z$	0.0427 0 −6.4770	2.0066	
		$f_{13} = z + x^2 - y^2$ (ES1d)	$y^2 - x^2 = z$	0.0183 0 −2.8219	2.0065	
ES2	$\dot{x} = f_{ij} \times (y)$ $\dot{y} = f_{ij} \times (-x + az)$ $\dot{z} = f_{ij} \times (by^2 - xz)$ $a = 1$ $b = 3$	$f_{20} = x$ (ES2a)	$(0, y, z)$	0.0644 0 −0.8279	2.0778	0.15 0 0.8
		$f_{21} = z$ (ES2b)	$(x, y, 0)$	0.0830 0 −1.0662	2.0778	
		$f_{22} = xz$ (ES2c)	$(0, y, z)$ $(x, y, 0)$	0.045417 0 −0.58463	2.0777	
		$f_{23} = 1 + x^2 - y^2$ (ES2d)	$y^2 - x^2 = 1$	0.16203 0 −0.2083	2.0778	
		$f_{24} = z + x^2 + y^2$ (ES2e)	$x^2 + y^2 = -z$	0.18284 0 −2.3481	2.0779	
		$f_{25} = z + x^2 - y^2$ (ES2f)	$y^2 - x^2 = z$	0.1398 0 −1.7931	2.0779	
ES3	$\dot{x} = f_{ij} \times (y^2 + axy)$ $\dot{y} = f_{ij} \times (-z)$ $\dot{z} = f_{ij} \times (b + xy)$ $a = 2$ $b = 1$	$f_{30} = x$ (ES3a)	$(0, y, z)$	0.0661 0 −1.664	2.0397	0.87 0.4 0
		$f_{31} = 34.81 - x^2 - y^2 - z^2$ (ES3b)	$x^2 + y^2 + z^2 = 34.81$	2.3995 0 −60.4616	2.0397	
		$f_{32} = 30.25 - x^2 - y^2$ (ES3c)	$x^2 + y^2 = 30.25$	2.1569 0 −54.3899	2.0397	
		$f_{33} = 1 + x^2 - 0.3460y^2$ (ES3d)	$0.3460y^2 - x^2 = 1$	0.0640 0 −1.6154	2.0397	

(*Continued*)

Table 1. (*Continued*)

Cases	System Structure	Introduced Functions	Surfaces of Equilibria	LEs	D_{KY}	(x_0, y_0, z_0)
ES4	$\dot{x} = f_{ij} \times (-y)$ $\dot{y} = f_{ij} \times (x + z)$ $\dot{z} = f_{ij} \times (ay^2 + xz - b)$ $a = 2$ $b = 0.35$	$f_{40} = z$ (ES4a)	$(x, y, 0)$	0.0560 0 −1.0855	2.0516	0 0.46 0.7
		$f_{41} = z + x^2 + y^2$ (ES4b)	$x^2 + y^2 = -z$	0.2330 0 −4.3048	2.0518	
ES5	$\dot{x} = f_{ij} \times (-az)$ $\dot{y} = f_{ij} \times (b + z^2 - xy)$ $\dot{z} = f_{ij} \times (x^2 - xy)$ $a = 0.4$ $b = 1$	$f_{50} = xy$ (ES5a)	$(0, y, z)$ $(x, 0, z)$	0.1242 0 −1.8356	2.0677	1 1.44 0
		$f_{51} = x$ (ES5b)	$(0, y, z)$	0.0987 0 −1.4578	2.0677	
		$f_{52} = y$ (ES5c)	$(x, 0, z)$	0.2613 0 −3.8683	2.0675	
		$f_{53} = z + x^2 + y^2$ (ES5d)	$x^2 + y^2 = -z$	0.2613 0 −3.8683	2.0675	
		$f_{54} = x^2 + y^2 + z^2 - 1$ (ES5e)	$x^2 + y^2 + z^2 = 1$	0.1819 0 −2.6959	2.0675	
		$f_{55} = x^2 + y^2 - 1$ (ES5f)	$x^2 + y^2 = 1$	0.1642 0 −2.4219	2.0678	
ES6	$\dot{x} = f_{ij} \times (y + ayz)$ $\dot{y} = f_{ij} \times (bz + y^2 + cz^2)$ $\dot{z} = f_{ij} \times (x^2 - y^2)$ $a = 2$ $b = 8$ $c = 7$	$f_{60} = xyz$ (ES6a)	$(0, y, z)$ $(x, 0, z)$ $(x, y, 0)$	0.0294 0 −0.4051	2.0725	1 −1.3 −1
		$f_{61} = x$ (ES6b)	$(0, y, z)$	0.1867 0 −2.5693	2.0727	
		$f_{62} = -y$ (ES6c)	$(x, 0, z)$	0.2327 0 −3.2026	2.0727	
		$f_{63} = -z$ (ES6d)	$(x, y, 0)$	0.0385 0 −0.5311	2.0725	
		$f_{64} = -xy$ (ES6e)	$(0, y, z)$ $(x, 0, z)$	0.2080 0 −2.8649	2.0726	
		$f_{65} = z + x^2 + y^2$ (ES6f)	$x^2 + y^2 = -z$	2.3535 0 −1.3994	2.0726	

Table 1. (*Continued*)

Cases	System Structure	Introduced Functions	Surfaces of Equilibria	LEs	D_{KY}	(x_0, y_0, z_0)
ES7	$\dot{x} = f_{ij} \times (ay)$ $\dot{y} = f_{ij} \times (xz)$ $\dot{z} = f_{ij} \times (-z - x^2 - byz)$ $a = 0.4$ $b = 6$	$f_{70} = 1 - x^2 - y^2 - z^2$ (ES7a)	$x^2 + y^2 + z^2 = 1$	0.0113 0 −0.9501	2.0119	0 0.1 0
		$f_{71} = 1 - x^2 - y^2$ (ES7b)	$x^2 + y^2 = 1$	0.0115 0 −0.9654	2.0119	
		$f_{72} = 1 + x^2 - y^2$ (ES7c)	$y^2 - x^2 = 1$	0.0124 0 −1.0416	2.0119	
ES8	$\dot{x} = f_{ij} \times (az + y^2)$ $\dot{y} = f_{ij} \times (-y + bx^2)$ $\dot{z} = f_{ij} \times (-xy)$ $a = 1$ $b = 5$	$f_{80} = 1 - x^2 - y^2 - z^2$ (ES8a)	$x^2 + y^2 + z^2 = 1$	0.0323 0 −0.9552	2.0338	0.24 0.2 0
		$f_{81} = 1 - x^2 - y^2$ (ES8b)	$x^2 + y^2 = 1$	0.0330 0 −0.9733	2.0339	
		$f_{82} = 1 + x^2 - y^2$ (ES8c)	$y^2 - x^2 = 1$	0.0348 0 −1.0261	2.0339	
ES9	$\dot{x} = f_{ij} \times (y^2 - axy)$ $\dot{y} = f_{ij} \times (xz)$ $\dot{z} = f_{ij} \times (1 - by^2)$ $a = 5$ $b = 7$	$f_{90} = 1 - x^2 - y^2$ (ES9a)	$x^2 + y^2 = 1$	0.0388 0 −1.2078	2.0321	0.06 0 1
		$f_{91} = x$ (ES9b)	$(0, y, z)$	0.0028 0 −0.0875	2.0318	
		$f_{92} = 1 + x^2 - y^2$ (ES9c)	$y^2 - x^2 = 1$	0.0399 0 −1.2485	2.0320	
ES10	$\dot{x} = f_{ij} \times (a - z^2)$ $\dot{y} = f_{ij} \times (xz)$ $\dot{z} = f_{ij} \times (y + bxz)$ $a = 0.1$ $b = 1$	$f_{10,0} = 1 + x^2 - y^2$ (ES10a)	$y^2 - x^2 = 1$	0.0420 0 −0.2330	2.1883	0 −0.08 0
		$f_{10,1} = 1 - x^2 - y^2 - z^2$ (ES10b)	$x^2 + y^2 + z^2 = 1$	0.0316 0 −0.1671	2.1891	
		$f_{10,2} = 1 - x^2 - y^2$ (ES10c)	$x^2 + y^2 = 1$	0.0364 0 −0.1938	2.1879	

(*Continued*)

Table 1. (*Continued*)

Cases	System Structure	Introduced Functions	Surfaces of Equilibria	LEs	D_{KY}	(x_0, y_0, z_0)
ES11	$\dot{x} = f_{ij} \times (yz)$ $\dot{y} = f_{ij} \times (x - axz)$ $\dot{z} = f_{ij} \times (x - bz^2)$ $a = 1$ $b = 0.6$	$f_{11,0} = z + x^2 + y^2$ (ES11a)	$x^2 + y^2 = -z$	0.0283 0 −0.6171	2.0458	0.46 0 0.8
		$f_{11,1} = 4.84 - x^2 - y^2 - z^2$ (ES11b)	$x^2 + y^2 + z^2 = 4.84$	0.1033 0 −2.2565	2.0458	
		$f_{11,2} = 4 - x^2 - y^2$ (ES11c)	$x^2 + y^2 = 4$	0.1047 0 −2.2891	2.0457	
		$f_{11,3} = 1 + x^2 - 0.25y^2$ (ES11d)	$0.25y^2 - x^2 = 1$	0.0375 0 −0.8180	2.0458	
ES12	$\dot{x} = f_{ij} \times (yz)$ $\dot{y} = f_{ij} \times (-ax)$ $\dot{z} = f_{ij} \times (-z + by^2 + xz)$ $a = 0.1$ $b = 6$	$f_{12,0} = z + x^2 - y^2$ (ES11a)	$y^2 - x^2 = z$	0.0068 0 −0.4998	2.0135	1 0 1
		$f_{12,1} = 1 + x^2 - y^2$ (ES12b)	$y^2 - x^2 = 1$	0.0165 0 −1.2226	2.0135	
		$f_{12,2} = z + x^2 + y^2$ (ES12c)	$x^2 + y^2 = -z$	0.0080 0 −0.5907	2.0136	

same core structure, including simple planes, a sphere, a circular cylinder, a hyperbolic cylinder, a paraboloid, and a saddle surface. All of the introduced equilibria exist outside the attractor without influencing the basic dynamics. For systems ES3b, ES3c, ES11b, and ES11c, the minimum radii are 5.9, 5.5, 2.2 and 2, respectively. The corresponding typical attractors with their corresponding equilibria are solved by the fourth-order Runge–Kutta method based on Matlab and are shown in Fig. 1. The time step is 0.005, and the data is 64-bit floating point number.

In fact, different equilibria can coexist in the same system if they do not intersect the attractor. For example, for the case of ES5, the newly introduced functions can be:

$$f_{56} = x(z + x^2 + y^2),$$

$$f_{57} = y(z + x^2 + y^2),$$

$$f_{58} = x(1 + x^2 - 0.3906y^2),$$

$$f_{59} = y(1 + x^2 - 0.3906y^2),$$

$$f_{5,10} = (z + x^2 + y^2)(1 + x^2 - 0.3906y^2),$$

$$f_{5,11} = xy(z + x^2 + y^2),$$

$$f_{5,12} = xy(1 + x^2 - 0.3906y^2),$$

$$f_{5,13} = x(z + x^2 + y^2)(1 + x^2 - 0.3906y^2),$$

$$f_{5,14} = y(z + x^2 + y^2)(1 + x^2 - 0.3906y^2) \quad \text{and}$$

$$f_{5,15} = xy(z + x^2 + y^2)(1 + x^2 - 0.3906y^2);$$

correspondingly, the derived systems share more than one surface of equilibria, as shown in Fig. 2. Offset boosting [Li *et al.*, 2019; Li *et al.*, 2018a; Li *et al.*, 2017b] can be applied to the original system to shift the attractor in case it touches the surface of equilibria.

In an extreme scenario, the expanded equilibria can form a solid space. Taking ES8 as an example; except for the isolated original equilibrium point, new functions can be introduced to embed infinitely many surfaces of equilibria and even a solid space. As shown in Table 2, the new function $\varphi(x)$ can be defined to introduce the equilibria of the solid

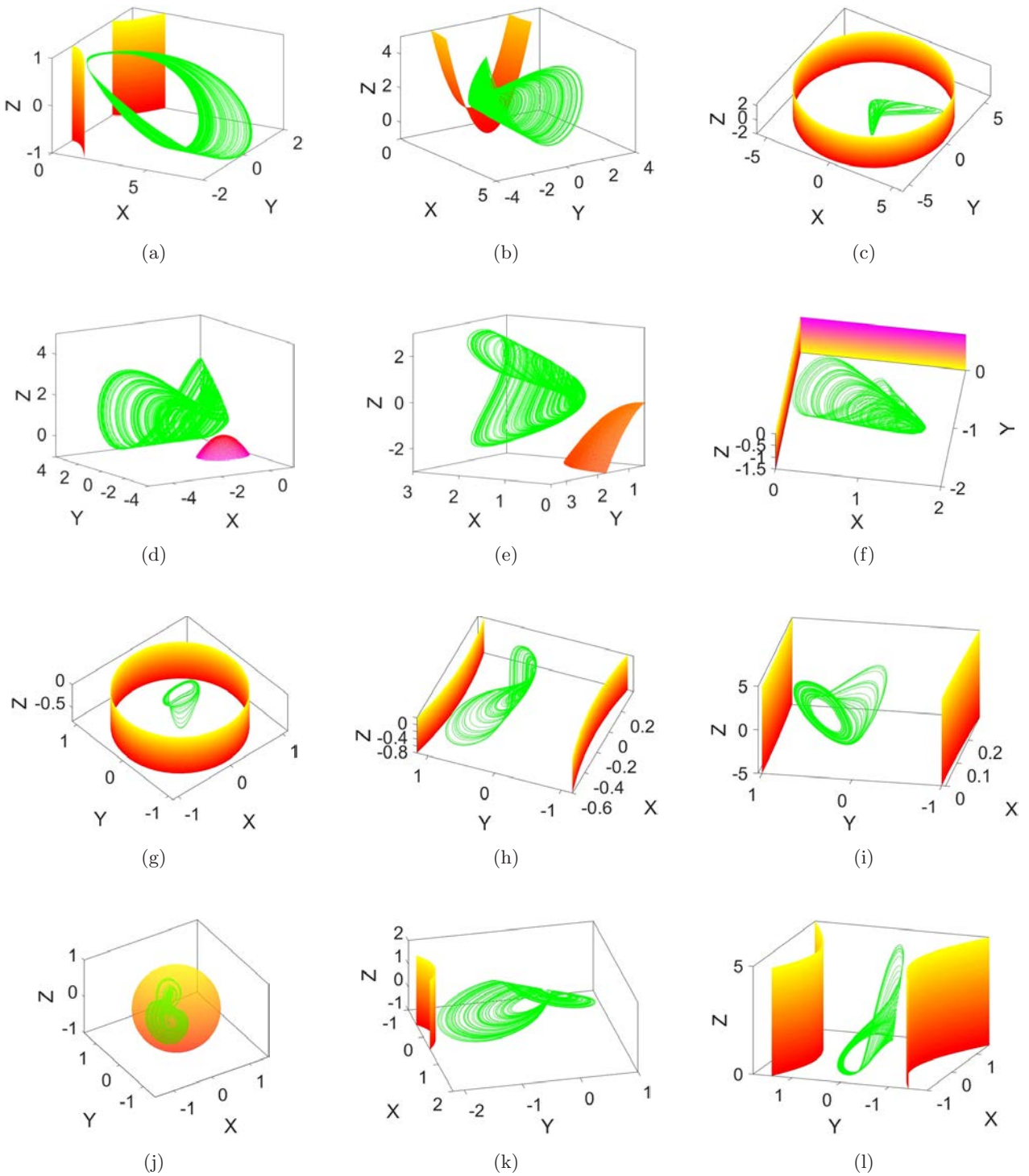

Fig. 1. Typical phase trajectories of the cases in Table 1. (a) ES1b, (b) ES2f, (c) ES3c, (d) ES4b, (e) ES5d, (f) ES6e, (g) ES7b, (h) ES8c, (i) ES9c, (j) ES10b, (k) ES11d, and (l) ES12b.

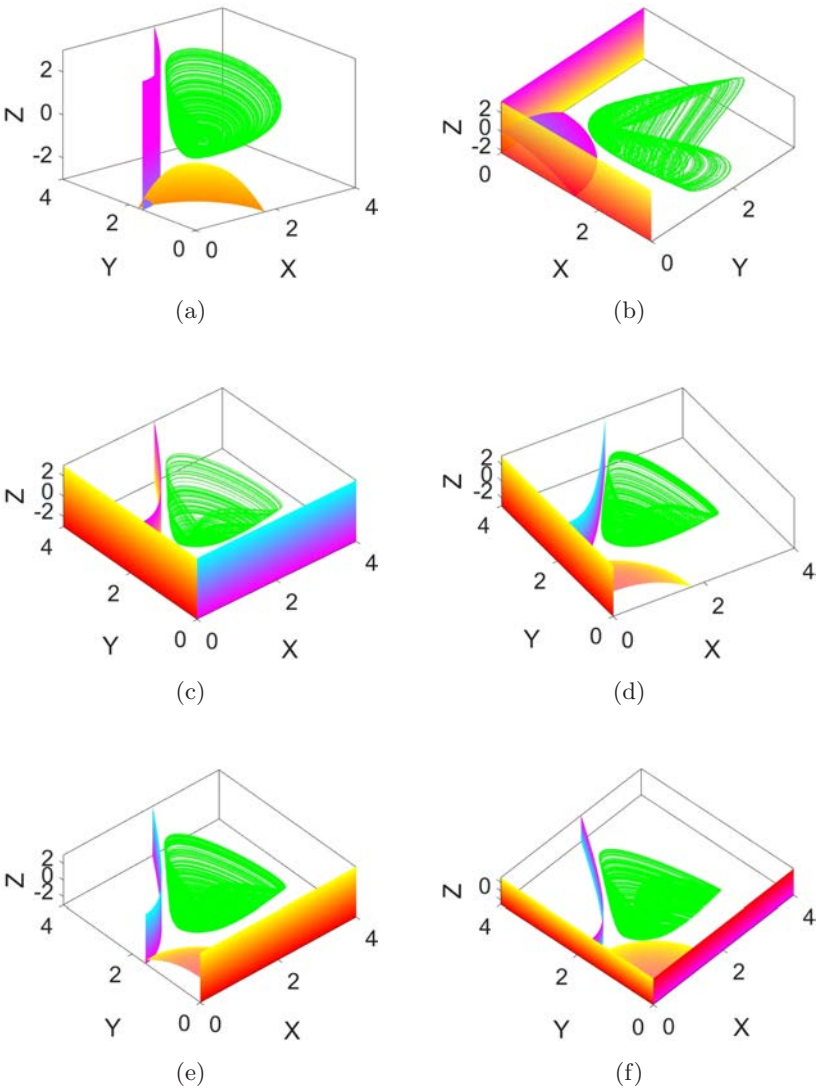

Fig. 2. Coexisting surfaces of equilibria and chaos in the case of ES5: (a) $f_{5,10}$, (b) $f_{5,11}$, (c) $f_{5,12}$, (d) $f_{5,13}$, (e) $f_{5,14}$ and (f) $f_{5,15}$.

Table 2. Chaotic flows induced from ES8 with a solid space of equilibria.

Case	System Structure	Introduced Functions	Surfaces of Equilibria	(x_0, y_0, z_0)
ES8	$\dot{x} = f_{ij} \times (az + y^2)$ $\dot{y} = f_{ij} \times (-y + bx^2)$ $\dot{z} = f_{ij} \times (-xy)$ $a = 1$ $b = 5$	$f_{83} = \varphi[-(x + 0.6)]$ (ES8d)	$x \leq -0.6$	0.24 0.2
		$f_{84} = \varphi[0.04 - (x + 0.6)^2 - y^2 - (z + 0.6)^2]$ (ES8e)	$(x + 0.6)^2 + y^2 + (z + 0.6)^2 \leq 0.04$	0
		$f_{85} = \varphi[0.04 - (x + 0.6)^2 - y^2]$ (ES8f)	$(x + 0.6)^2 + y^2 \leq 0.04$	
		$f_{86} = \varphi[-(1 + x^2 - y^2)]$ (ES8g)	$y^2 - x^2 \geq 1$	

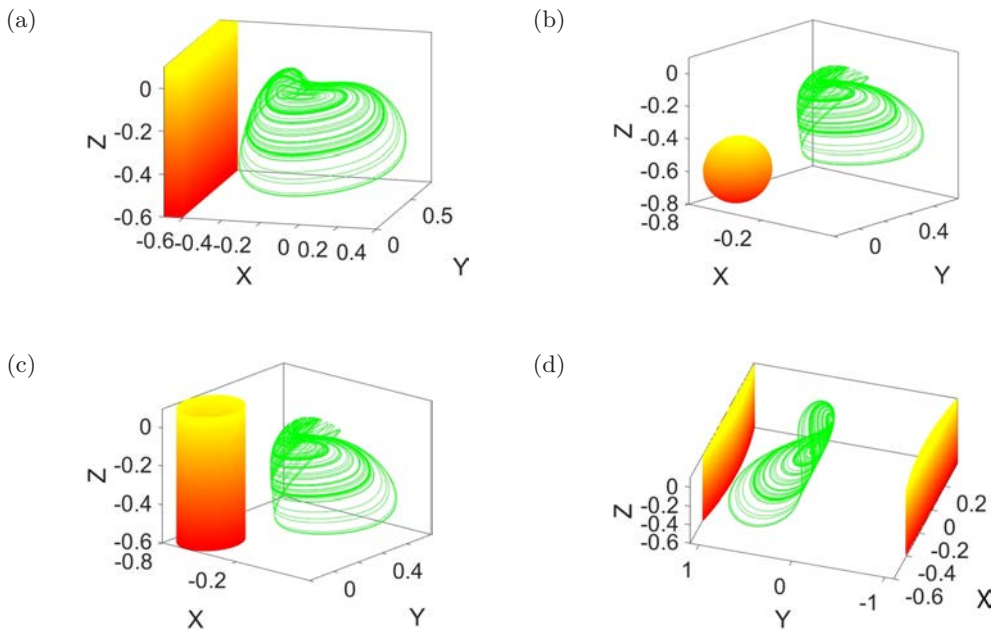

Fig. 3. Coexisting solid space of equilibria and chaos in the case of ES8: (a) ES8d, (b) ES8e, (c) ES8f and (d) ES8g.

space,

$$\varphi(x) = \begin{cases} 0, & x \geq 0, \\ 1, & x < 0. \end{cases} \tag{1}$$

Therefore, a cubic, sphere, cylinder, or even a hyperboloid space of equilibria can be planted into the body of chaotic systems, whose phase trajectories and equilibria are shown in Fig. 3. Furthermore, if $f_{ij} = 1$, all of the core systems share the same shapes of the chaotic attractor.

Similarly, lines of equilibria can be introduced in chaotic systems. Taking ES5 as an example,

$$\begin{cases} \dot{x} = x \times (-az) \\ \dot{y} = y \times (b + z^2 - xy) \\ \dot{z} = y \times (x^2 - xy) \end{cases} \tag{2}$$

$$\begin{cases} \dot{x} = \text{sgn}[x(x+1)] \times (-az) \\ \dot{y} = \text{sgn}[y(y+1)] \times (b + z^2 - xy) \\ \dot{z} = \text{sgn}[y(y+1)] \times (x^2 - xy). \end{cases} \tag{3}$$

The corresponding phase trajectories are shown in Fig. 4. Here, in the above systems (2) and (3), the newly introduced functions in three dimensions are different, and usually the signum function is used to remove the amplitude information [Li & Sprott, 2017]. Surfaces of equilibria can be introduced to the chaotic flows with a line of equilibria [Jafari & Sprott, 2013b]. Taking LE1 as an example,

$$\begin{cases} \dot{x} = g_i \times (y), \\ \dot{y} = g_i \times (-x + yz), \\ \dot{z} = g_i \times (-x - axy - bxz). \end{cases} \tag{4}$$

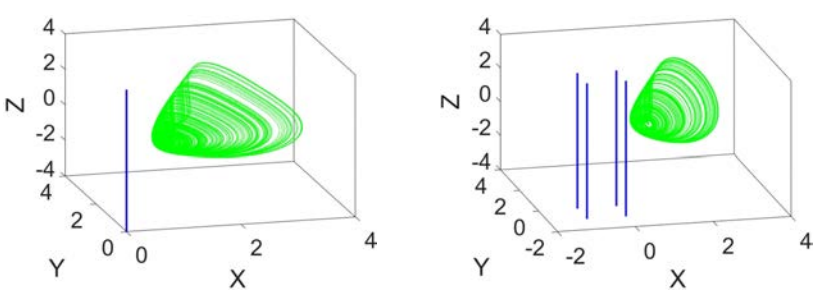

(a) (b)

Fig. 4. Coexisting lines of equilibria and chaos in the derived system of ES5: (a) System (2) and (b) system (3).

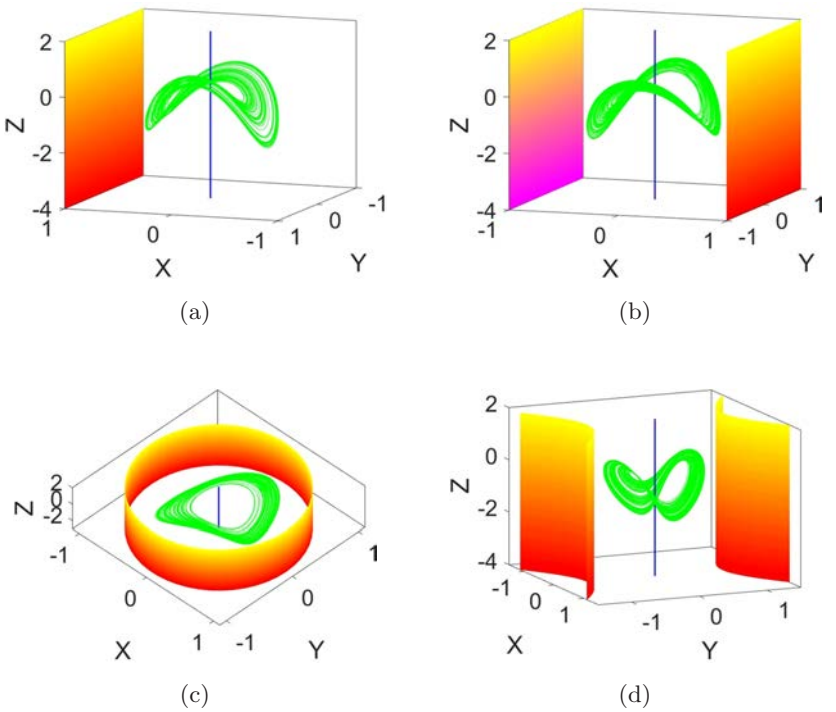

Fig. 5. Coexisting line and surface of equilibria and chaos of system (4): (a) Surface $x = 1$, (b) surface $x = \pm 1$, (c) surface $x^2 + y^2 = 1$ and (d) surface $y^2 - x^2 = 1$.

When $g_i = 1 - x, 1 - x^2, x^2 + y^2 - 1, 1 + x^2 - y^2$, coexisting surfaces of equilibria are introduced in the chaotic flow with a line of equilibria, as shown in Fig. 5.

3. Frequency Control and Dynamical Analysis

As conjectured, the derived flows with different types of equilibria exhibit almost the same fundamental dynamical behavior. The introduced equilibria result from the unified functions in all dimensions. Generally, for a dynamical system such as

$$\dot{X} = F(X), \quad X = (x_1, x_2, \ldots, x_n)^{\mathrm{T}},$$
$$F = (f_1, f_2, \ldots, f_n)^{\mathrm{T}},$$
$$\dot{X} = (\dot{x}_1, \dot{x}_2, \ldots, \dot{x}_n)^{\mathrm{T}}$$
$$= \left(\frac{dx_1}{dt}, \frac{dx_2}{dt}, \ldots, \frac{dx_n}{dt}\right)^{\mathrm{T}},$$

a positive real constant c in the differential equation $\dot{X} = cF(X)$ only introduces a time scaling since the transformation $t \to \frac{t}{c}$ can restore the equation to its original form. The function in the equation $\dot{X} = g(X)F(X)$ produces a surface of equilibria $g(X) = 0$ and simultaneously modifies the frequency and revises the dynamics accordingly. Taking system ES5 as an example, the projection of the chaotic attractor is located in the first quadrant in the x–y plane; therefore, we introduce a flexible offset-boostable plane in the core structure ES5 as follows:

$$\begin{cases} \dot{x} = (x - d) \times (-az) \\ \dot{y} = (x - d) \times (b + z^2 - xy) \\ \dot{z} = (x - d) \times (x^2 - xy). \end{cases} \tag{5}$$

When the distance between the attractor and the plane $x = d$ varies, the frequency of the chaotic oscillation is nearly linearly rescaled, and finally, the system ends in a limit cycle as shown in Fig. 6. Another plane $y = d$ produces the same influence as shown in Fig. 7 when it is introduced in the core system ES5:

$$\begin{cases} \dot{x} = (y - d) \times (-az), \\ \dot{y} = (y - d) \times (b + z^2 - xy), \\ \dot{z} = (y - d) \times (x^2 - xy). \end{cases} \tag{6}$$

The effect of the surface of equilibria can be clearly identified by the offset d in the function $f = x - d$. When the offset d increases from -2 to 0.8,

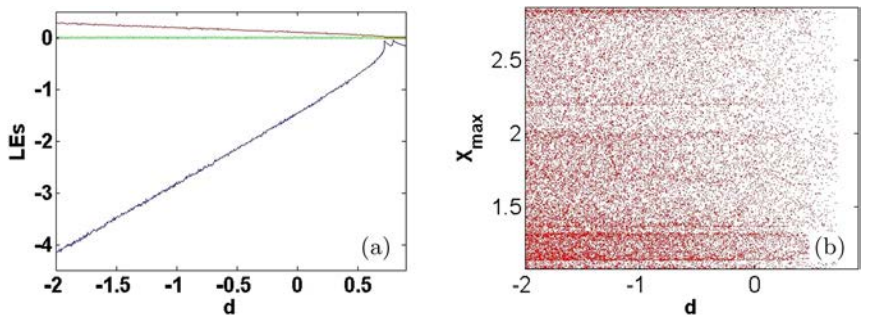

Fig. 6. Dynamical evolution of system (5) under the plane of $x = d$: (a) Lyapunov exponents and (b) bifurcation diagram.

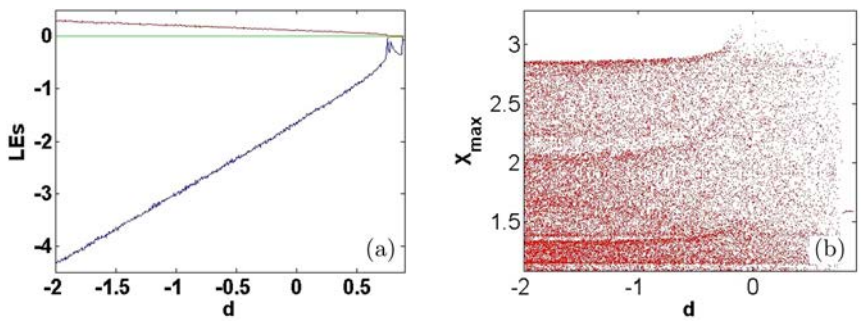

Fig. 7. Dynamical evolution of system (6) under the plane of $y = d$: (a) Lyapunov exponents and (b) bifurcation diagram.

systems (5) and (6) remain dominantly chaotic with linearly rescaled Lyapunov exponents and finally end in a periodic oscillation. A larger Lyapunov exponent indicates a high frequency as shown in Fig. 8. The effect of the frequency rescaling can be enlarged by the power function. When $f = x, x^2, x^3$, the frequency is modified in the positive correlation shown in Fig. 9. The offset in the z-dimension

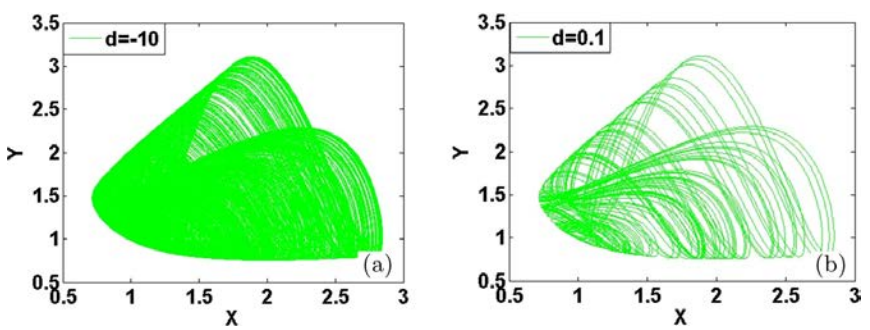

Fig. 8. Phase trajectory of system (5) with $a = 0.4$ and $b = 1$ in the $x - y$ plane: (a) $d = -10$ and (b) $d = 0.1$.

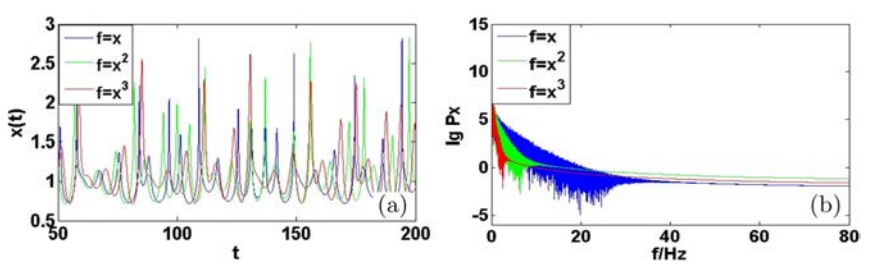

Fig. 9. Frequency rescaled by power functions in system ES5 with $a = 0.4$ and $b = 1$: (a) Chaotic signal of $x(t)$ and (b) frequency spectrum of $x(t)$.

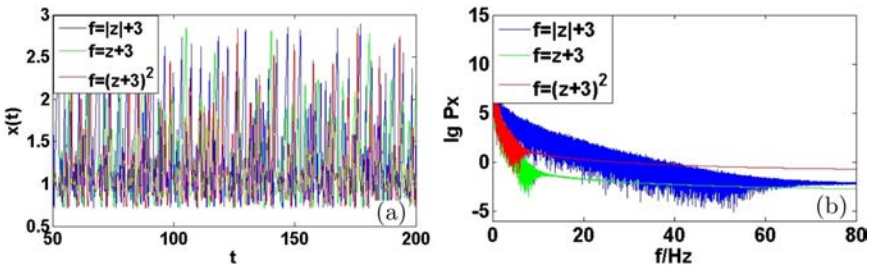

Fig. 10. Frequency rescaled by other offset-boosted planes in system ES5 with $a = 0.4$ and $b = 1$: (a) Chaotic signal of $x(t)$ and (b) frequency spectrum of $x(t)$.

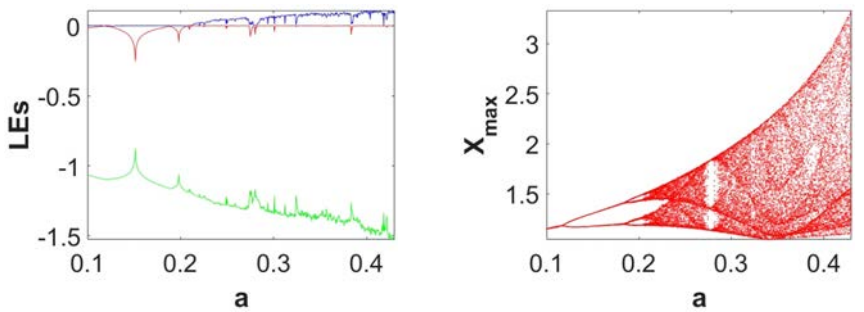

(a) (b)

Fig. 11. Lyapunov exponents and bifurcation diagram of chaotic system ES5a.

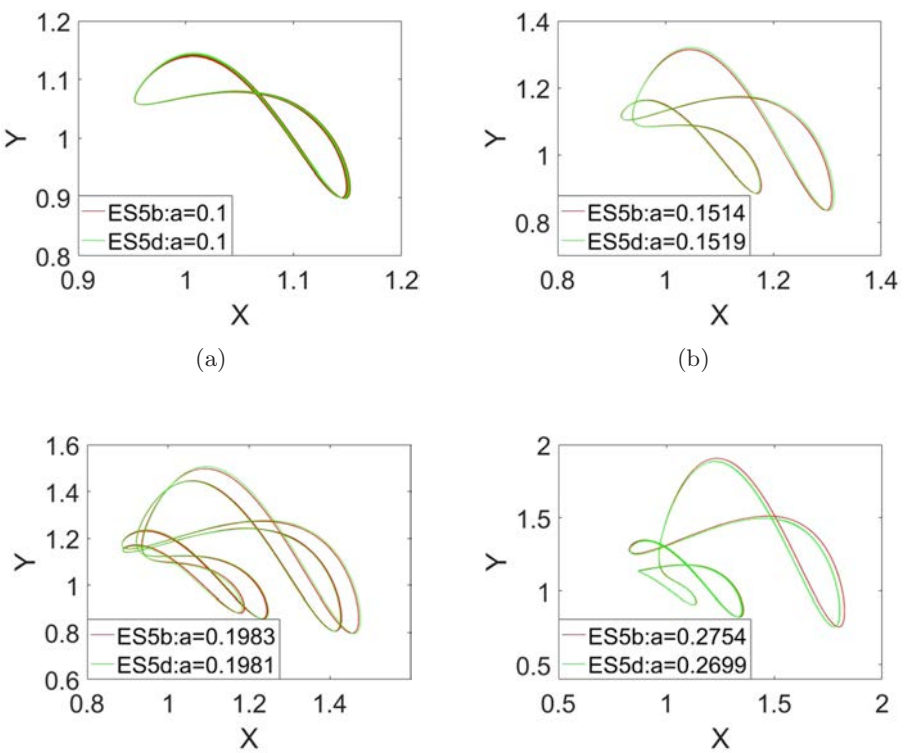

(a) (b) (c) (d)

Fig. 12. Simultaneously appearing periodic oscillations in systems ES5b and ES5d.

can also produce surfaces of equilibria when $f = |z| + 3, z + 3, (z + 3)^2$, providing frequency rescaling as shown in Fig. 10.

For the fixed surfaces of equilibria, taking ES5 as an example, all of the systems exhibit a similar period-doubling bifurcation as shown in Fig. 11. Specifically, limit cycles appear almost in the same periodic windows. Period-1, period-2, period-4, and period-3 cycles appear simultaneously in systems ES5b and ES5d as shown in Fig. 12. Furthermore, it is found that many of these cases with surfaces of equilibria exhibit the same fundamental dynamics when the equilibria are removed.

4. Circuit Implementation

To verify the chaotic flows with surfaces of equilibria, electrical circuit simulations were carried out as follows. Taking system ES5d as an example, a circuit schematic is designed as shown in Fig. 13, and the circuit equation is

$$\begin{cases} \dot{x} = f \times \dfrac{R_2}{R_4 C_1}\left(-\dfrac{1}{R_3} z\right), \\ \dot{y} = f \times \dfrac{R_7}{R_9 C_2}\left(\dfrac{1}{R_{11}} + \dfrac{1}{R_8} z^2 - \dfrac{1}{R_{12}} xy\right), \\ \dot{z} = f \times \dfrac{R_{14}}{R_{16} C_3}\left(\dfrac{1}{R_{15}} x^2 - \dfrac{1}{R_{18}} xy\right), \\ f = R_{20}\left(\dfrac{R_1}{R_5 R_{22}} x^2 + \dfrac{R_6}{R_{10} R_{21}} y^2 + \dfrac{R_{13}}{R_{17} R_{19}} z\right). \end{cases} \tag{7}$$

Here, the parameters are set as $R_1 = R_3 = R_4 = R_5 = R_6 = R_7 = R_8 = R_9 = R_{10} = R_{11} = R_{12} = R_{13} = R_{14} = R_{15} = R_{16} = R_{17} = R_{18} = R_{19} = R_{20} = R_{21} = R_{22} = 10\,\text{k}\Omega$, $R_2 = 4\,\text{k}\Omega$ and $C_1 = C_2 = C_3 = 100\,\text{nF}$. Small capacitor values are selected for suitable time rescaling. The initial values are 1 V, 1.44 V, and 0 V, respectively. All the operational amplifiers are LM741H, which are powered with $V_{CC} = 15\,\text{V}$ and $V_{EE} = -15\,\text{V}$. For the

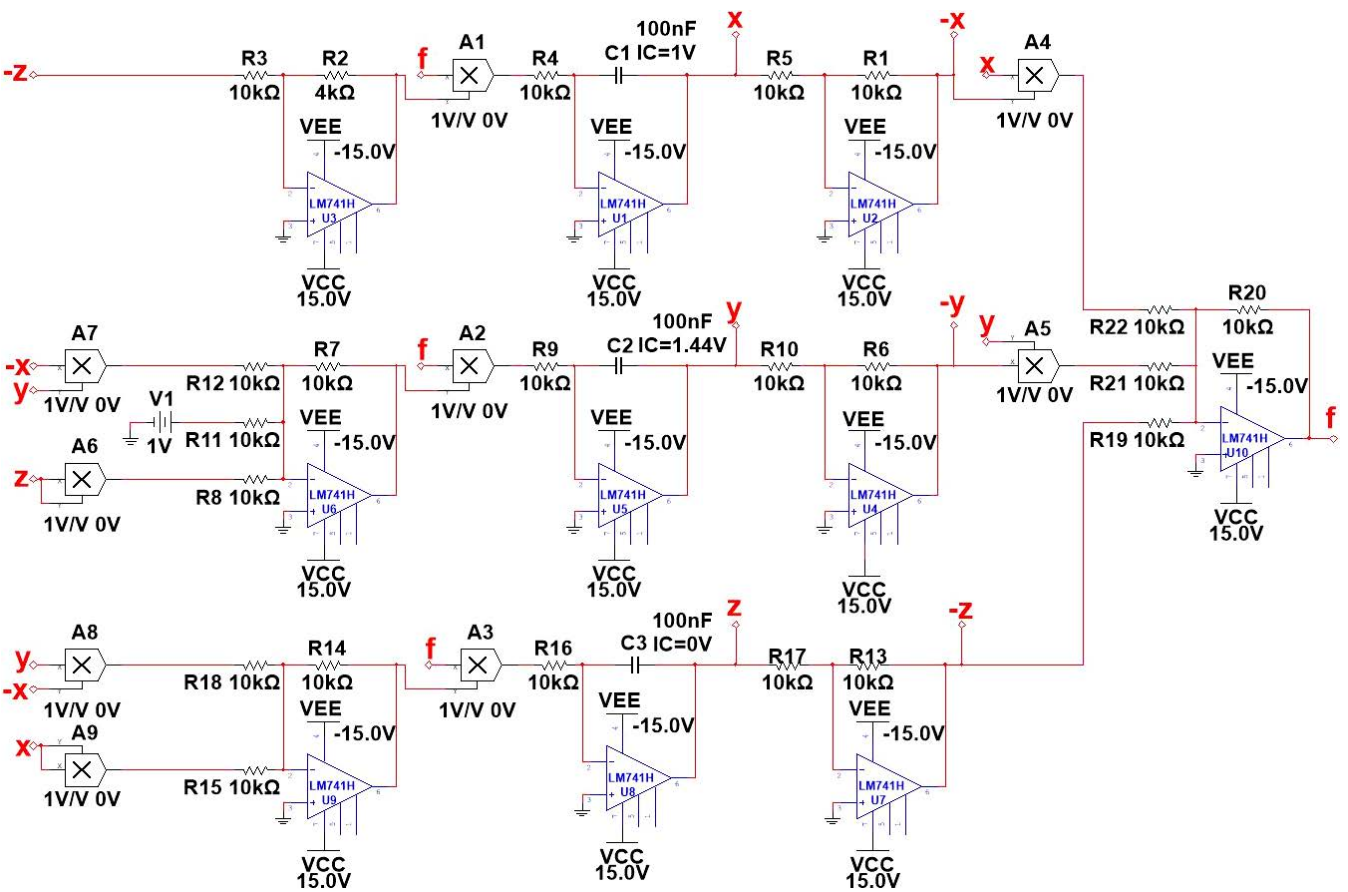

Fig. 13. Circuit schematic of system ES5d.

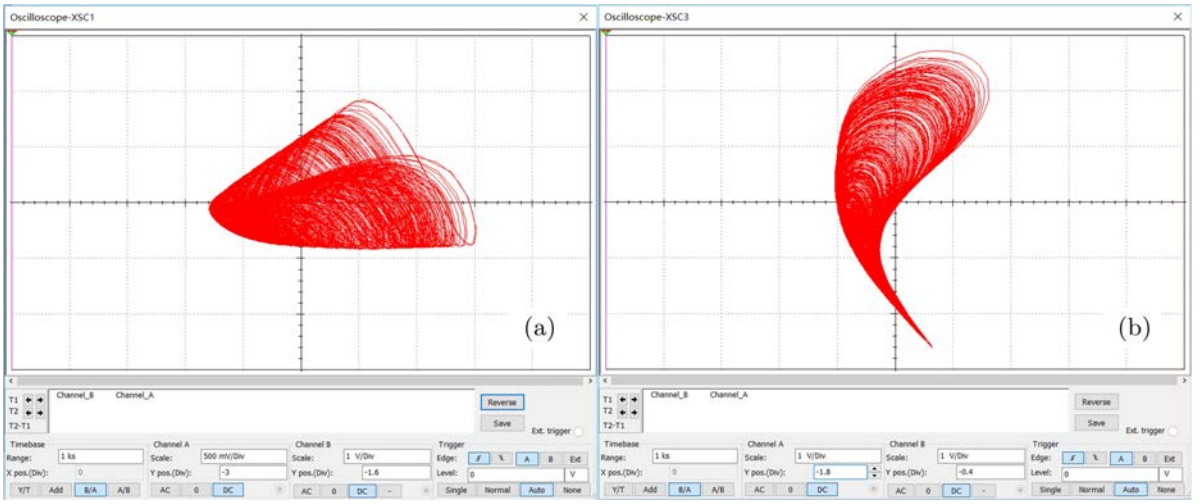

Fig. 14. Phase trajectory of system ES5d on the oscilloscope: (a) x–y plane and (b) y–z plane.

multiplier, the scaling parameters are $A_1 = A_2 = A_3 = A_4 = A_5 = 1\,\mathrm{V/V}$. The newly introduced equilibria become a "wall" of multipliers, which introduces feedback into the core structure. In fact, this wall of equilibria does not influence the attractor while providing a new parasitic position for the system when the initial conditions are present. The phase trajectory of system ES5d on the oscilloscope is shown in Fig. 14.

To observe the influence of the distance between the surface of equilibria and the attractor, an offset-boostable plane is introduced in the core system ES5. The corresponding circuit schematic is designed as shown in Fig. 15, and the circuit

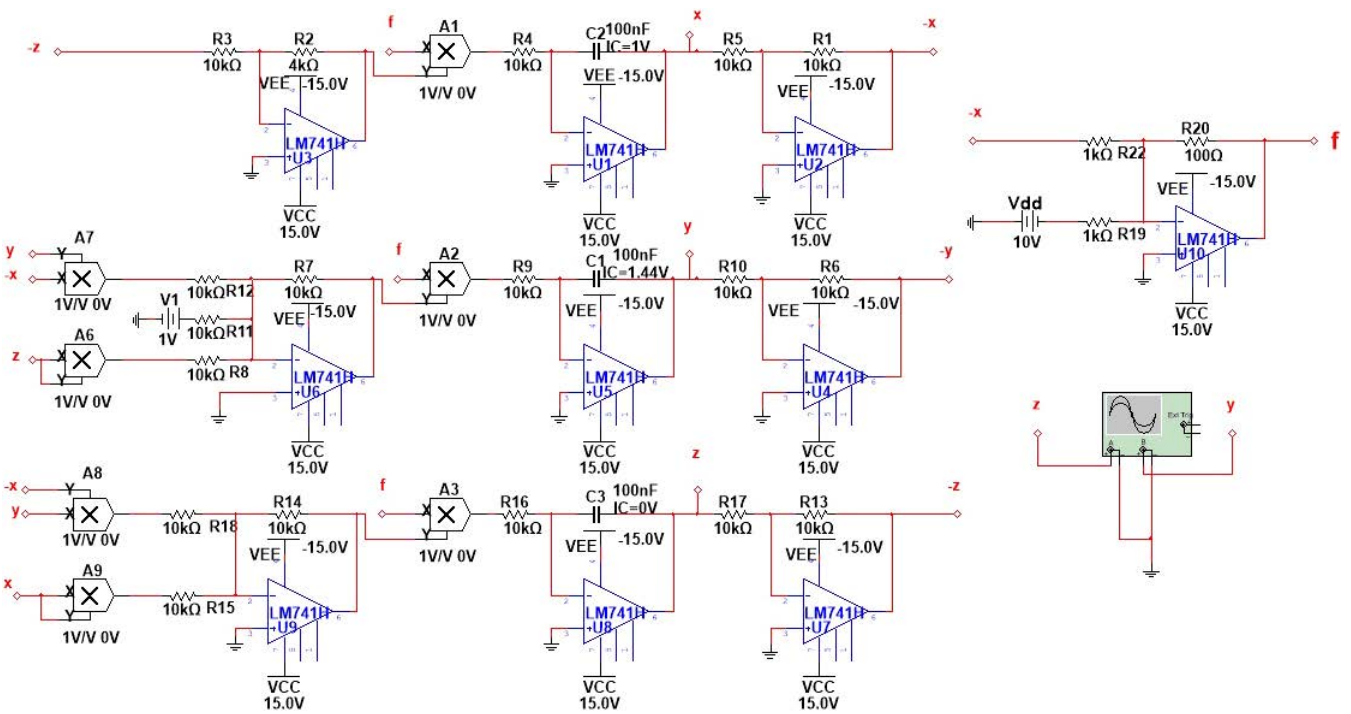

Fig. 15. Circuit schematic of system (5).

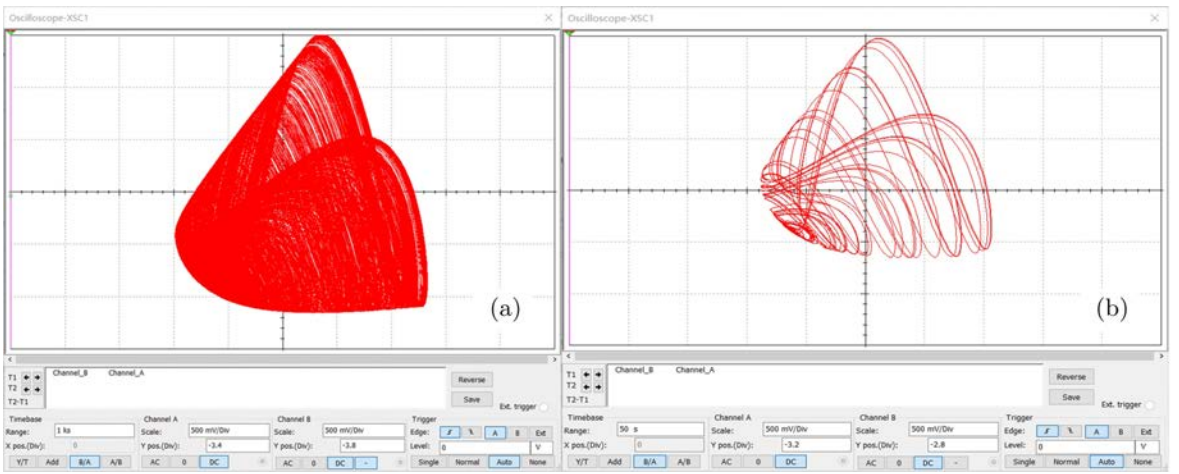

Fig. 16. Phase trajectory of system (5) on the simulated oscilloscope in the x–y plane: (a) $R_{19} = R_{20} = R_{22} = 1\,\mathrm{k}\Omega$, and $V_{dd} = -10$ and (b) $R_{19} = R_{20} = R_{22} = 100\,\Omega$, and $V_{dd} = 0.1$.

equation is

$$\begin{cases} \dot{x} = f \times \dfrac{R_2}{R_4 C_1}\left(-\dfrac{1}{R_3}z\right), \\ \dot{y} = f \times \dfrac{R_7}{R_9 C_2}\left(\dfrac{1}{R_{11}} + \dfrac{1}{R_8}z^2 - \dfrac{1}{R_{12}}xy\right), \\ \dot{z} = f \times \dfrac{R_{14}}{R_{16} C_3}\left(\dfrac{1}{R_{15}}x^2 - \dfrac{1}{R_{18}}xy\right), \\ f = R_{20}\left(\dfrac{R_1}{R_5 R_{22}}x - \dfrac{R_1}{R_5 R_{19}}V_{dd}\right). \end{cases} \tag{8}$$

Here, the parameters are set as $R_1 = R_3 = R_4 = R_5 = R_6 = R_7 = R_8 = R_9 = R_{10} = R_{11} = R_{12} = R_{13} = R_{14} = R_{15} = R_{16} = R_{17} = R_{18} = R_{19} = R_{22} = 10\,\mathrm{k}\Omega, R_2 = 4\,\mathrm{k}\Omega$ and $C_1 = C_2 = C_3 = 100\,\mathrm{nF}$. Select $R_{19} = R_{20} = R_{22} = 100\,\Omega$ and $R_{19} = R_{20} = R_{22} = 1\,\mathrm{k}\Omega$ for different offset-boosting. As shown in Fig. 8, it is clear that the frequency of the chaotic attractor of system (5) is modified accordingly. A larger offset produces a higher frequency as shown in Fig. 16.

5. Conclusion and Discussion

Chaotic systems with infinitely many equilibria are discussed in this paper. Specifically, extra functions are introduced in the differential equation in a unified or slightly different manner to construct lines, surfaces, or even a solid space of equilibria. Following this method, additional cases of chaotic systems with surfaces, lines or even a solid space of equilibria are constructed based on the previously found elegant flows. In fact, if the surface does not intersect the existing attractor in the core structure, any desired equilibria of a particular type can be introduced into the core structure. Note that for considering dynamical systems generated by ODEs, their limit objects (like attractors) and limit quantities (like LEs and D_{KY}) should be investigated, and one should study the existence and uniqueness of ODE solutions and extensibility of these solutions over time to positive infinity [Kuznetsov *et al.*, 2018; Leonov *et al.*, 2015]. In this work many of those induced systems are artificially constructed with continuous yet nonsmooth functions in their right-hand side (such as the function in Eq. (1), or the absolute value function) and even discontinuous signum functions, further investigation on Lipschitz condition or the boundedness of solutions is suggested in the future for ensuring that the ODEs indeed generate dynamical systems.

Offset-boosting makes the surface farther from or closer to the attractor in the core system, providing time rescaling, which influences the frequency without changing the basic dynamics. Newly equipped surfaces of equilibria can be introduced and superimposed, which provides an additional parameter to vary. A bifurcation analysis shows that the fundamental dynamics are almost independent of the newly introduced infinite equilibria in some circumstances. Dynamical maps or basins of attraction analysis are suggested to enhance this claim for further exploration. The circuit simulations agree with the numerical simulation. The possible practical application of the developed systems is that in such systems those newly

equipped surfaces of equilibria can be applied for controlling the system to various stabilities.

Acknowledgments

This work was supported financially by the National Natural Science Foundation of China (Grant Nos. 61871230 and 61971228), the Natural Science Foundation of Jiangsu Province (Grant No. BK20181410), and a project funded by the Priority Academic Program Development of Jiangsu Higher Education Institutions (PAPD).

Conflict of Interest

The authors declare that they have no conflict of interest.

References

Akgul, A., Calgan, H., Koyuncu, I., Pehlivan, I. & Istanbullu, A. [2016] "Chaos-based engineering applications with a 3D chaotic system without equilibrium points," *Nonlin. Dyn.* **84**, 481–495.

Bao, B., Jiang, T., Xu, Q., Chen, M., Wu, H. & Hu, Y. [2016] "Coexisting infinitely many attractors in active band-pass filter-based memristive circuit," *Nonlin. Dyn.* **86**, 1711–1723.

Bao, B., Jiang, T., Wang, G., Jin, P., Bao, H. & Chen, M. [2017] "Two-memristor-based Chua's hyperchaotic circuit with plane equilibrium and its extreme multistability," *Nonlin. Dyn.* **89**, 1–15.

Deng, Q. & Wang, C. [2019] "Multi-scroll hidden attractors with two stable equilibrium points," *Chaos* **29**, 093112.

Ekmekci, A. & Rockwell, D. [2010] "Effects of a geometrical surface disturbance on flow past a circular cylinder: A large-scale spanwise wire," *J. Fluid Mech.* **665**, 120–157.

Jafari, S. & Sprott, J. C. [2013a] "Elementary quadratic chaotic flows with no equilibria," *Phys. Lett. A* **377**, 699–702.

Jafari, S. & Sprott, J. C. [2013b] "Simple chaotic flows with a line equilibrium," *Chaos Solit. Fract.* **57**, 79–84.

Jafari, S., Pham, V. T. & Kapitaniak, T. [2016a] "Multiscroll chaotic sea obtained from a simple 3D system without equilibrium," *Int. J. Bifurcation and Chaos* **26**, 1650031-1–7.

Jafari, S., Sprott, J. C. & Molaie, M. [2016b] "A simple chaotic flow with a plane of equilibria," *Int. J. Bifurcation and Chaos* **26**, 1650098-1–6.

Jafari, S., Sprott, J. C., Pham, V. T., Volos, C. & Li, C. [2016c] "Simple chaotic 3D flows with surfaces of equilibria," *Nonlin. Dyn.* **86**, 1–10.

Kuznetsov, A. P., Kuznetsov, S. P., Mosekilde, E. & Stankevich, N. V. [2013] "Generators of quasiperiodic oscillations with three-dimensional phase space," *Eur. Phys. J. Special Topics* **222**, 2391–2398.

Kuznetsov, N. V., Leonov, G. A., Mokaev, T. N., Prasad, A. & Shrimali, M. D. [2018] "Finite-time Lyapunov dimension and hidden attractor of the Rabinovich system," *Nonlin. Dyn.* **92**, 267–285.

Lai, Q. & Chen, S. [2016] "Generating multiple chaotic attractors from Sprott B system," *Int. J. Bifurcation and Chaos* **26**, 1650177-1–13.

Leonov, G. A., Vagaitsev, V. I. & Kuznetsov, N. V. [2011] "Localization of hidden Chua's attractors," *Phys. Lett. A* **375**, 2230.

Leonov, G. A., Vagaitsev, V. I. & Kuznetsov, N. V. [2012] "Hidden attractor in smooth Chua systems," *Physica D* **241**, 1482.

Leonov, G. A. & Kuznetsov, N. V. [2013a] "Hidden attractors in dynamical systems from hidden oscillations in Hilbert–Kolmogov, Aizerman, and Kalman problems to hidden chaotic attractors in Chua circuits," *Int. J. Bifurcation and Chaos* **23**, 1330002-1–69.

Leonov, G. A. & Kuznetsov, N. V. [2013b] *Prediction of Hidden Oscillations Existence in Nonlinear Dynamical Systems*: *Analytics and Simulation* (Springer International Publishing).

Leonov, G. A., Kuznetsov, N. V. & Mokaev, T. N. [2015] "Homoclinic orbits, and self-excited and hidden attractors in a Lorenz-like system describing convective fluid motion," *Eur. Phys. J. Special Topics* **224**, 1421.

Li, C. & Sprott, J. C. [2013] "Multistability in a butterfly flow," *Int. J. Bifurcation and Chaos* **23**, 1350199-1–10.

Li, C. & Sprott, J. C. [2014] "Chaotic flows with a single nonquadratic term," *Phys. Lett. A* **378**, 178–183.

Li, C., Sprott, J. C. & Thio, W. [2014] "Bistability in a hyperchaotic system with a line equilibrium," *J. Exp. Theor. Phys.* **118**, 494–500.

Li, C., Sprott, J. C. & Thio, W. [2015a] "Linearization of the Lorenz system," *Phys. Lett. A* **379**, 888–893.

Li, C., Sprott, J. C., Yuan, Z. & Li, H. [2015b] "Constructing chaotic systems with total amplitude control," *Int. J. Bifurcation and Chaos* **25**, 1530025-1–14.

Li, C. & Sprott, J. C. [2017] "How to bridge attractors and repellors," *Int. J. Bifurcation and Chaos* **27**, 1750149-1–11.

Li, C., Sprott, J. C. & Xing, H. [2017a] "Constructing chaotic systems with conditional symmetry," *Nonlin. Dyn.* **87**, 1351–1358.

Li, C., Wang, X. & Chen, G. [2017b] "Diagnosing multistability by offset boosting," *Nonlin. Dyn.* **90**, 1335–1341.

Li, C., Sprott, J. C., Liu, Y., Gu, Z. & Zhang, J. [2018a] "Offset boosting for breeding conditional symmetry," *Int. J. Bifurcation and Chaos* **28**, 1850163-1–13.

Li, C., Thio, J. C., Sprott, J. C., Iu, H. H. C. & Xu, Y. [2018b] "Constructing infinitely many attractors in a programmable chaotic circuit," *IEEE Access* **6**, 29003–29012.

Li, C., Lu, T., Chen, G. & Xing, H. [2019] "Doubling the coexisting attractors," *Chaos* **29**, 051102.

Ma, J., Chen, Z., Wang, Z. & Zhang, Q. [2015] "A four-wing hyper-chaotic attractor generated from a 4D memristive system with a line equilibrium," *Nonlin. Dyn.* **81**, 1275–1288.

Maaita, J., Volos, C. K., Kyprianidis, I. & Stouboulos, I. [2015] "The dynamics of a cubic nonlinear system with no equilibrium point," *J. Nonlin. Dyn.* **2015**, 257923.

Macbeath, A. M. [1965] "Geometrical realization of isomorphisms between plane groups," *Bull. Amer. Math. Soc.* **71**, 629–630.

Molaie, M. & Jafari, S. [2013] "Simple chaotic flows with one stable equilibrium," *Int. J. Bifurcation and Chaos* **23**, 1350188-1–7.

Wang, X. & Chen, G. [2013] "Constructing a chaotic system with any number of equilibria," *Nonlin. Dyn.* **71**, 429–436.

Yang, Q. & Chen, G. [2008] "A chaotic system with one saddle and two stable node foci," *Int. J. Bifurcation and Chaos* **18**, 1393–1414.

Zhang, X. & Wang, C. [2019a] "Multiscroll hyper-chaotic system with hidden attractors and its circuit implementation," *Int. J. Bifurcation and Chaos* **29**, 1950117-1–14.

Zhang, X. & Wang, C. [2019b] "A novel multi-attractor period multi-scroll chaotic integrated circuit based on CMOS wide adjustable CCCII," *IEEE Access* **7**, 16336–16350.

Zhou, L., Wang, C. & Zhou, L. [2018] "A novel no-equilibrium hyperchaotic multi-wing system via introducing memristor," *Int. J. Circ. Th. Appl.* **46**, 84–98.